Vol. 405: 131–145, 2010
doi: 10.3354/meps08497

MARINE ECOLOGY PROGRESS SERIES
Mar Ecol Prog Ser

Published April 29

OPEN ACCESS

Relationships among upwelling, phytoplankton blooms, and phycotoxins in coastal Oregon shellfish

J. F. Tweddle[1,10,*], P. G. Strutton[1], D. G. Foley[2,3], L. O'Higgins[4], A. M. Wood[5,6], B. Scott[5,11], R. C. Everroad[5,12], W. T. Peterson[7], D. Cannon[8], M. Hunter[9], Z. Forster[9]

[1]College of Oceanic and Atmospheric Science, Oregon State University, 104 COAS Admin Bldg, Corvallis, Oregon 97331, USA
[2]NOAA Fisheries, Southwest Fisheries Science Center, 1352 Lighthouse Ave, Pacific Grove, California 93950, USA
[3]Joint Institute for Marine and Atmospheric Research, University of Hawaii, 1000 Pope Rd, Honolulu, Hawaii 96822, USA
[4]Cooperative Institute for Marine Research Studies, Hatfield Marine Science Center, 2030 Marine Science Drive, Newport, Oregon 97365, USA
[5]Center for Ecology and Evolutionary Biology, University of Oregon, Eugene, Oregon 97403, USA
[6]Atlantic Oceanographic and Meterological Laboratory, NOAA, Miami, Florida 33129, USA
[7]NOAA Northwest Fisheries Science Centre, Newport Research Station — Bldg 955, 2032 SE OSU Drive, Newport, Oregon 97365, USA
[8]Oregon Department of Agriculture, 635 Capitol St. NE, Salem, Oregon 97301-2532, USA
[9]Oregon Department of Fish and Wildlife, 2001 Marine Drive, Astoria, Oregon 97103, USA

[10]*Present address:* Department of Earth Sciences, Boston University, 675 Commonwealth Ave Rm 141, Boston, Massachusetts 02215, USA

[11]*Present address:* Nelson Laboratories, 6280 South Redwood Road, Salt Lake City, Utah 84123, USA

[12]*Present address:* RIKEN Advanced Science Institute, Yokohama 230-0045, Japan

ABSTRACT: Climatologies derived from satellite data (1998 to 2007) were used to elucidate seasonal and latitudinal patterns in winds, sea surface temperature (SST), and chlorophyll concentrations (chl) over the Oregon shelf. These were further used to reveal oceanographic conditions normally associated with harmful algal blooms (HABs) and toxic shellfish events along the Oregon coast. South of 43° N, around Cape Blanco, summer upwelling started earlier and finished later than north of 43° N. Spring blooms occur when light limitation is relieved, before the initiation of upwelling, and secondary, more intense blooms occur approximately 2 wk after upwelling is established. North of 45° N, SST and chl are heavily influenced by the Columbia River plume, which delays upwelling-driven cooling of the surface coastal ocean in spring, and causes phytoplankton blooms (as indicated by increased chl) earlier than expected. The presence of saxitoxin in coastal shellfish, which causes paralytic shellfish poisoning, was generally associated with late summer upwelling. The presence of domoic acid in shellfish, which leads to amnesic shellfish poisoning, was greatest during the transition between upwelling and downwelling regimes. This work demonstrates that satellite data can indicate physical situations when HABs are more likely to occur, thus providing a management tool useful in predicting or monitoring HABs.

KEY WORDS: Oregon coast · California Current · Upwelling · Bloom timing · Harmful algae · Paralytic shellfish poisoning · Domoic acid poisoning · Saxitoxin

INTRODUCTION

The west coast of the USA, including Oregon, has experienced a marked increase in algal blooms, harmful and benign, over the last 10 to 15 yr (Anderson et al. 2008, Kahru & Mitchell 2008, Kahru et al. 2009). The frequency, persistence, toxicity, and geographical extent of harmful algal blooms (HABs) are increasing worldwide (Landsberg 2002). Possible explanations range from natural mechanisms of species dispersal to a host of human-related phenomena, such as nutrient enrichment (Parsons & Dortch 2002, Glibert et al.

*Email: jtweddle@bu.edu

2005), climatic shifts, or transport of algal species via ship ballast (Smayda 2007).

Blooms of species belonging to the diatom genus *Pseudo-nitzschia* Peragallo, which contains many producers of the toxin domoic acid, have been repeatedly documented along the Pacific coast of the USA (Fryxell et al. 1997, Horner et al. 1997). Horner et al. (1997) summarized the known history of domoic acid in coastal waters off the west coast of the USA. In Oregon and Washington, domoic acid was first detected in 1991, following seabird deaths in California, which led to the closing of shellfish and crab fisheries in November of that year (Wood et al. 1993). Phycotoxins such as domoic acid can enter the food chain through consumption of toxic algae by, for example, zooplankton and filter-feeding organisms such as mussels. In 1998, California sea lions were killed by domoic acid poisoning (Scholin et al. 2000), and high levels of domoic acid were subsequently found in Washington razor clams (Adams et al. 2000). In recent years, particularly 2003, 2004, and 2005, domoic acid contamination has resulted in spatially large and prolonged closures of Oregon razor clam and mussel beds to harvesting, with financial costs estimated at US $4.8 million for the 2003 closure (Oregon Department of Fish and Wildlife [ODFW] unpubl. estimate).

Clamming is closed seasonally on the Clatsop Beaches (northern Oregon) between 15 July and 30 September; however, Oregon shellfish beds coastwide are also often closed due to clams or mussels accumulating saxitoxin (Scott 2007), a neurotoxin that can cause paralysis and death in humans (Shumway 1990). These closures are linked to the presence of toxic dinoflagellates in the water column, specifically *Alexandrium catenella* (Whedon & Kofold) Balech (Horner et al. 1997, Horner 2001). Domoic acid and saxitoxin cause amnesic shellfish poisoning (ASP) and paralytic shellfish poisoning (PSP) in humans, respectively.

Oregon coastal waters are part of the California Current system, with mostly wind driven dynamics over the continental shelf (for a comprehensive review, see Barth & Wheeler 2005 and papers in the associated special volume). In winter, westerly and southwesterly winds and storms drive downwelling and mixing over the shelf, whereas in summer, southward winds drive upwelling via Ekman transport (Huyer et al. 1979). The spring transition between winter downwelling conditions and summer upwelling is associated with an increase in chlorophyll (chl) concentrations (Thomas & Strub 1989, Thomas et al. 1994, Henson & Thomas 2007), which lasts through the upwelling season. Spatial and temporal resolution of seasonal cycles along the Oregon coast has generally been lacking in previous work. This study makes use of multi-year climatologies of satellite-derived parameters to determine latitudinal variations in the initiation of upwelling/downwelling favorable winds in spring/autumn, and associated sea surface temperature (SST) and chl signals.

To minimize the human health and economic impacts of HABs in Oregon and elsewhere, monitoring programs that can provide accurate information to coastal managers are essential. These monitoring programs will be most effective and efficient if they are informed by science regarding the locations of HABs and the timing of their onset and demise in relation to environmental cues and non-toxic algal blooms. The impetus for the research presented here was to develop a tool capable of warning coastal managers of potential toxic events in shellfish through the use of satellites. The analysis presented here compares mean seasonal cycles of upwelling and chl to counts of toxic algae and the concentrations of toxins in shellfish, to relate HABs to general oceanographic conditions along the Oregon coast. The genera *Pseudo-nitzschia* and *Alexandrium* Halim have no optically unique identifiers for use with current satellites. Therefore, satellite color, or chl, data alone are unlikely to identify HABs. However, when combined with knowledge of the location and timing of HAB events in relation to other events such as upwelling, satellite imagery could provide some early warning to coastal managers that conditions are favorable to HAB development.

The data presented here identify a latitudinal gradient in the onset and intensity of upwelling along the Oregon coast. The timing of upwelling initiation and termination was analyzed in relation to the occurrence of potentially toxic species and toxins in coastal water samples, providing a framework of environmental data within which to interpret HAB data. Regions and time periods of frequent toxin occurrence are identified, and opportunities for future research and monitoring programs are discussed.

MATERIALS AND METHODS

Study region. The Oregon coast was divided into 5 regions, of 1° latitude and 0.5° longitude. The regions were chosen to provide insight into timing of HABs and occurrences of toxic shellfish along the coast, in the context of seasonal cycles in ocean physics and biology. The 5 regions facilitate relevant interpretation of results for coastal management, but were not of sufficiently small scale to investigate specific toxin events. From north to south, these regions were named A, B, C, D, and E (Fig. 1, Table 1). Five oceanic regions, with 1° latitude ranges corresponding to the coastal regions and a width of 1° longitude (128.5 to 127.5° W), were

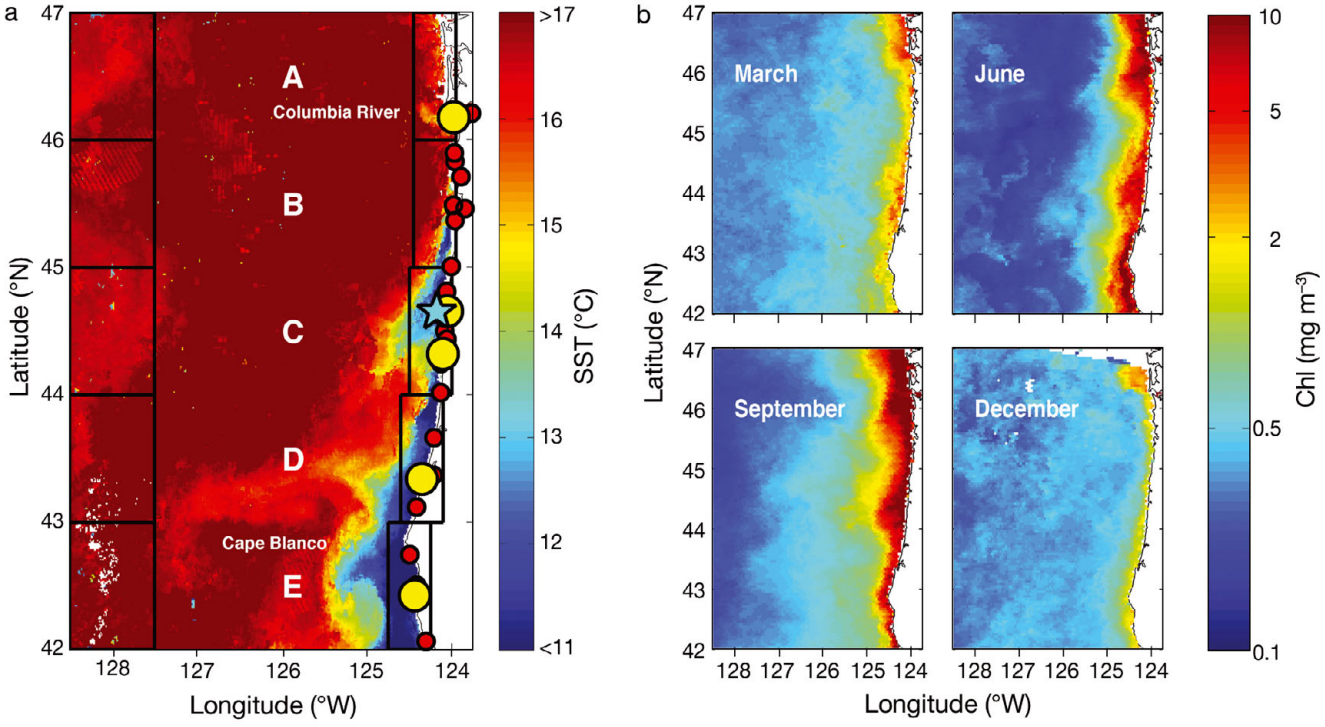

Fig. 1. Oregon coast, with (a) AVHRR 8 d mean sea surface temperature (SST, °C) from 3 August 2007 (27 July to 3 August, period of upwelling), and (b) monthly climatologies of MODIS chlorophyll concentrations (mg m^{-3}). Boxes in (a) mark the study region boundaries. Small red circles indicate the positions of Oregon Department of Agriculture sampling sites, larger yellow circles show Oregon Department of Fish and Wildlife sampling sites, and the star is sampling site NH5

Table 1. Boundaries of regions and locations of study sites depicted in Fig. 1(a). Letters A through E refer to the coastal and oceanic box dimensions. Both latitude and longitude are given for the coastal boxes. Latitudes for the oceanic boxes are the same as for the corresponding coastal boxes, and longitudes for the oceanic boxes are all 128.5° to 127.5° W. The last 4 columns give names and locations of Oregon Department of Fish and Wildlife (ODFW) 2005 to 2007 sampling sites

Study region	Latitudes (°N)	Coastal longitudes (°W)	ODFW reference name	Site	Latitude (°N)	Longitude (°W)
A	46–47	124.45–123.95	Clatsop	Clatsop Beach at Gerhardt	46.176	123.976
B	45–46	124.45–123.95	Lincoln	–	–	–
C	44–45	124.50–124.00	Lane	Agate Beach	44.655	124.055
				Bob Creek	44.320	124.104
D	43–44	124.60–124.10	Coos	Bastendorff Beach	43.340	124.350
E	42–43	124.75–124.25	Curry	Bailey Beach	42.425	124.434

also designated. These offshore data were compared to the coastal data to isolate variability in the coastal signal due to upwelling and large-scale seasonality.

Satellite analyses. Level 3 Advanced Very High Resolution Radiometer (AVHRR) SST, SeaWiFS chl *a* concentration, and QuikSCAT wind stress and direction were obtained from the National Oceanic and Atmospheric Administration (NOAA) CoastWatch West Coast Regional Node, for the years 1998 to 2007 (from 1999 for QuikSCAT). Data were supplied as a running average of 8 d means in an attempt to minimize loss of coverage due to clouds. SST data were available for ~89% of days, chl for 92%, and wind for 86%. AVHRR and SeaWiFS pixel resolution was 0.0125°, and QuikSCAT resolution was 0.25°. The satellite data had a cloud mask applied. The data were spatially averaged to give a mean parameter value for each of the 5 coastal region boxes per day. For comparison of coastal and offshore dynamics, equivalent SST and chl means for the oceanic regions were obtained in the same manner as the coastal regions. A 'detrended' coastal SST (ΔSST) was obtained by subtracting each region's oceanic SST from the corresponding coastal SST, for each day of each year, removing the seasonal heating cycle from the coastal data. This analysis also provided a measure of upwelling impact within each

region, that is, the seasonally detrended ΔSST data included the effects of upwelling but not the latitudinal gradients and seasonal cycles in heating and cooling. Therefore, negative values of ΔSST would be considered indicative of upwelling-induced cooling at the coast. Note that this detrended value is not the anomaly from the climatological seasonal cycle. SST can be affected by cloud contamination, such as by cloud edges, sub-pixel and thin clouds, producing anomalously low temperature values. Temporal and spatial averaging minimized the effect of this, as did visual identification and subsequent removal of any atypically low values. An annual climatology of each parameter, for each study region along the coast, was calculated as the mean for each year day (1–365 or 366) across all years.

Minimum and maximum yearly values for each parameter (e.g. SST_{min} and SST_{max}) were calculated as the mean of the 10 lowest and highest values, respectively, for each year. QuikSCAT winds were separated into north–south and east–west vectors, and $wind_{max}$ and $wind_{min}$ were calculated for the north–south component (most relevant to upwelling). Bloom conditions were defined as chl concentrations 5% greater than the annual median concentration (Siegel et al. 2002, Henson et al. 2006a,b, Henson & Thomas 2007). The start of bloom conditions was therefore the first day of the year that chl exceeded this value.

Upwelling indices. Mean daily upwelling indices for 3 latitudes (42°, 45°, and 48° N) along the coast were obtained for 1998 to 2007 from the NOAA Southwest Fisheries Science Center, Environmental Research Division (ERD, Live Access Server 2008, NOAA Southwest Fisheries Science Center: www.pfeg.noaa.gov/products/las.html). Data were derived from synoptic (6 hourly) sea level pressure gridded fields by ERD, and are reported as a single climatology for all years.

***In situ* sampling.** The Oregon Department of Agriculture (ODA), and the ODFW collect shellfish tissue and water samples, respectively, at sites along the Oregon coast, shown in Fig. 1. For analysis, data from these *in situ* sources were grouped into the study region (A through E) from which they came.

ODA provided domoic acid and saxitoxin concentration data from intertidal shellfish. Samples were obtained from a variety of shellfish (mussels, razor clams, eastern thin-shelled clams, cockles, and oysters), depending on presence and accessibility, between 1979 and 2007 and between 1994 and 2007 for saxitoxin and domoic acid, respectively. Site locations and frequency of sampling varied throughout the time series, based on the specific needs and capabilities of ODA for the given sampling year, species, or site. Samples were separated into the 5 coastal regions. Saxitoxin concentrations were measured using the standard mouse bioassay method (AOAC 1990). Domoic acid concentrations were measured using high performance liquid chromatography (HPLC) methods recommended by the Canadian Food Inspection Agency's Shellfish Sanitation Program[1]. Detection levels varied slightly for saxitoxin due to the method of detection, but were generally between 32 and 38 µg 100 g^{-1} extracted shellfish tissue. Domoic acid detection levels were 1 ppm. Closure levels are considered 80 µg 100 g^{-1} for saxitoxin, and 20 ppm for domoic acid.

The ODA sampling program was recently augmented by surf zone sampling for phytoplankton conducted by ODFW scientists at 5 sites, beginning in 2005 (Fig. 1, Table 1), and increasing to 12 sites in 2008. The ODFW provides cell counts of *Pseudo-nitzschia* spp. and *Alexandrium* spp. These counts were obtained from whole water plankton samples taken throughout the year, generally every 2 wk, conditions permitting, and allowed to settle overnight. After a 10-fold reduction, the live samples were loaded into a Palmer-Maloney slide (a nanoplankton counting chamber of 0.1 ml) and allowed to settle for 5 min, and the entire chamber was counted at 20× magnification.

In addition to the ODFW sampling, surface water samples were collected weekly or biweekly from 2001 to 2005, weather dependent, at site NH5 (Fig. 1) on the Newport Hydrographic Line, and a sub-sample preserved in a solution of Lugol's Iodine. A 50 ml aliquot was examined under an inverted phase contrast microscope at a magnification of 20×. Cell counts of *Alexandrium* spp. and *Pseudo-nitzschia* spp. were taken. In this analysis, cells were sorted only to genus level.

From these 3 types of *in situ* sampling (shellfish toxicity, surf-zone net tows, and NH5 surface samples), monthly climatological values of toxicity and species cell concentrations were calculated, and the 95% confidence intervals of these values were calculated using bootstrapping (Efron & Gong 1983).

Columbia River data. Columbia River discharge data were also acquired, because the river has been shown to influence the physical environment of the northern Oregon and southern Washington coast (Thomas & Weatherbee 2006). River temperature data at Camas/Washougal, Washington (45.58° N, 122.38° W) were obtained from the University of Washington's Columbia Basin Research, Columbia River Data Access in Real Time (DART 2008, www.cbr.washington.edu/dart/dart.html) for 1998 to 2007. River discharge data were obtained from the United States Geological Survey (USGS) National Water Information System (http://waterdata.usgs.gov/nwis) for the same time period.

[1]Method disseminated at the 1992 Washington Sea Grant Program, Workshop on Momoic Acid, Seattle, WA

Statistics. Data were tested for significant differences (for example, differences in SST between regions, or toxin concentrations between months) using analysis of variance (ANOVA), with an α of 0.05 (95% confidence level). Whenever data are stated as significantly different, ANOVA returned $F > F_{crit}$ and $p < 0.05$.

RESULTS

Spatial and temporal variability in SST describes the seasonal and latitudinal variability of the physical environment to which potentially harmful algal blooms are subjected. SST from the oceanic regions showed a seasonal trend at all study latitudes (Fig. 2a). Minimum oceanic SST (SST_{min}) occurred in mid-March (~20 March) and decreased significantly to the north (Table 2). The timing of the onset of spring warming was not significantly different between regions. In the summer, oceanic SST reached a maximum (SST_{max}) in all regions. The southern regions, C, D, and E, reached SST_{max} on 24 August (± 4 d), and there was no significant difference in SST_{max} between these regions (Table 2). SST_{max} was significantly cooler for Regions A and B, and occurred on 31 August (± 4 d; 1 wk later than the southern regions). This oceanic SST represents the seasonal cycle of warming and cooling, without coastal processes such as upwelling.

SST in the coastal regions also displayed spring warming and autumnal cooling (Fig. 2b); however, the signal was not as well defined as in the corresponding oceanic regions. Summer warming was 'dampened' due to upwelling. The dampening of the signal was progressively stronger to the south, with the least seasonal variation apparent in Region E. Coastal summer SST_{max} (Table 2) was warmer to the north. SST_{max} values in Regions A and B were not significantly different, but SST_{max} values were significantly cooler with each region to the south. In winter, in Regions C to A, coastal SST_{min} (Table 2) significantly decreased northward. Coastal SST_{min} of Regions C, D, and E were not significantly different.

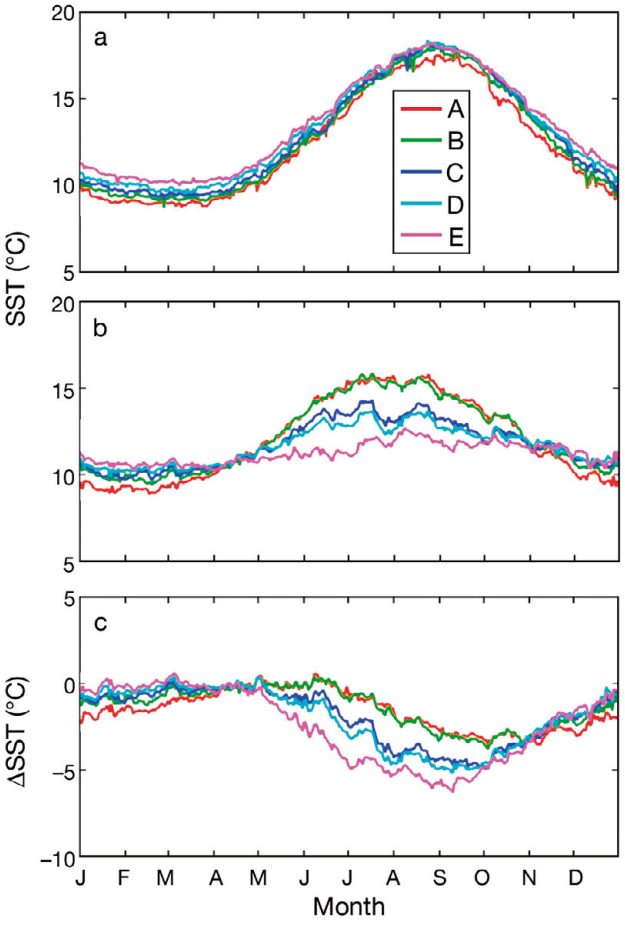

Fig. 2. Mean daily sea surface temperature (SST,°C) from (a) oceanic and (b) coastal study regions (A to E, see Fig.1), and (c) mean daily detrended sea surface temperature (ΔSST, coastal SST–oceanic SST), 1998 to 2007

In winter, ΔSST (Fig. 2c) was significantly different among all regions, becoming less negative to the south. In all regions, ΔSST increased slightly through the spring season, reaching a maximum (ΔSST_{max}, Table 2) before cooling over summer. The onset of cooling was calculated as when there was a 5% decrease from

Table 2. Maximum and minimum sea surface temperatures (SST,°C, ± 95% CI, as calculated from multi-year time series), for the oceanic and coastal regions, and detrended coastal SST. The date of cooling (± 95% CI, in days) is taken to be when there is a 5% decrease from ΔSST_{max}

Study region	Oceanic		Coastal		Detrended		Cooling
	SST_{max}	SST_{min}	SST_{max}	SST_{min}	ΔSST_{max}	ΔSST_{min}	
A	17.8 ± 0.15	8.4 ± 0.14	16.7 ± 0.11	8.6 ± 0.21	2.1 ± 0.12	−3.4 ± 0.16	26 May ± 14
B	18.1 ± 0.13	8.7 ± 0.18	16.7 ± 0.13	9.2 ± 0.12	2.0 ± 0.12	−4.2 ± 0.12	27 May ± 23
C	18.4 ± 0.14	9.0 ± 0.14	15.5 ± 0.17	9.4 ± 0.14	1.8 ± 0.18	−5.9 ± 0.10	31 Mar ± 17
D	18.5 ± 0.12	9.4 ± 0.11	15.0 ± 0.19	9.5 ± 0.17	1.5 ± 0.10	−6.4 ± 0.12	31 Mar ± 23
E	18.4 ± 0.12	9.8 ± 0.12	14.0 ± 0.17	9.3 ± 0.13	1.1 ± 0.13	−6.9 ± 0.09	24 Feb ± 26

ΔSST_{max}, after the maxima had occurred, for all years in each region. This date was not significantly different between Regions A and B (26–27 May), but was significantly earlier in Regions C and D (31 March), and E (24 February). In summer, ΔSST_{min} (Table 2) decreased significantly southward with each region.

A major driving force of the oceanographic physical environment along the Oregon coast is wind. Wind stress exhibited a seasonal cycle (Fig. 3), with winds to the north (downwelling favorable) dominating during winter, and winds to the south (upwelling favorable) dominating during summer. There was no significant difference between adjoining regions in the magnitude of $wind_{max}$ (greatest northward wind stress, Table 3), although $wind_{max}$ slightly increased southward, resulting in a significant decrease in $wind_{max}$ between regions D and A. $Wind_{max}$ occurred around 4 January in all regions in all years.

Periods of southward, upwelling favorable winds were similar between all regions. The upwelling season was considered to have begun when winds were to the south for 10 out of 14 d (Henson & Thomas 2007). There was no significant difference in the timing of the first upwelling event (considered the start of the upwelling season) between regions (Table 3), with 22 February as the mean start date. However, winds were more consistently and strongly southward in Region E than other regions during the first few months of the upwelling season. This is reflected in the climatology becoming consistently upwelling favorable significantly earlier in Region E than in the other regions (Fig. 3). With the exception of Regions B and C, all regions exhibited significantly different $wind_{min}$ (greatest southward wind stress, Table 3), with Region E in particular showing much stronger winds to the south in summer. $Wind_{min}$ was centered around 19 July in all regions. The upwelling season was considered to have finished when winds were to the north, i.e. downwelling favorable, for 10 out of 14 d. There was no significant difference in the timing of the end of upwelling between Regions A through D (10 November, Table 3). Region E switched to downwelling significantly later in the year than other regions, on 7 December.

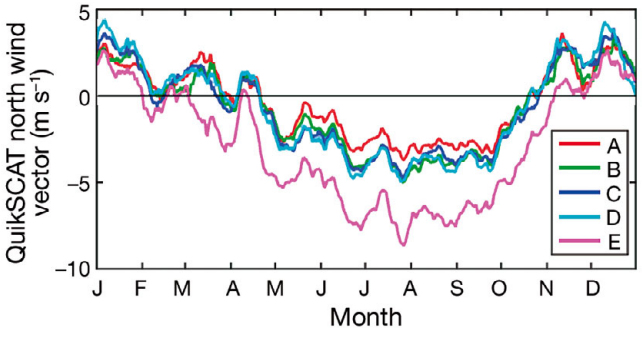

Fig. 3. Mean daily north–south wind stress vector (m s^{-1}), from the coastal study regions (A to E, see Fig.1), 1999 to 2007 (smoothed with a 20 d moving average)

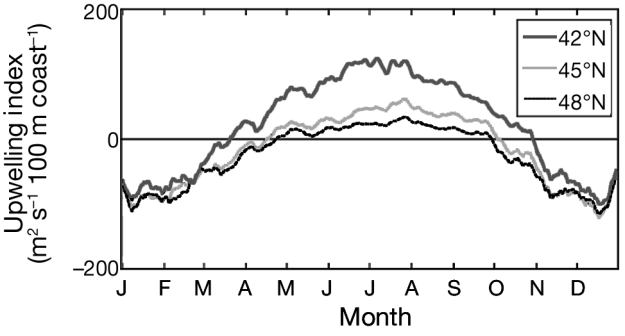

Fig. 4. Mean daily coastal upwelling indices at 42°, 45°, and 48° N, 1998 to 2007. Data derived from synoptic (6 hourly) sea level pressure gridded fields. From NOAA Environmental Research Division

Negative upwelling indices, indicating downwelling, occurred during winter (November to February) at all 3 latitudes (Fig. 4). Summer upwelling, indicated by a positive upwelling index, started progressively later to the north (Table 4): 5 March at 42° N, 12 March at 45° N, and 4 April at 48° N. Upwelling ended progressively later to the south: 9 November, 18 October, and 15 October, respectively. The maximum strength of upwelling was significantly weaker in the north ($upwelling_{max}$, Table 4) and remained weaker throughout the upwelling season. These results are broadly consistent with the corresponding analysis of the wind data.

Columbia River discharge was highest in May and June, and lowest during September (Fig. 5). A seasonal cycle was apparent in the temperature data, with temperatures lowest in winter (January/February) and highest in summer (July/August).

Table 3. Maximum and minimum north–south wind vectors (m s^{-1}, ± 95% CI, as calculated from multi-year time series), for the oceanic and coastal regions, and date (± CI, in days) of spring upwelling and autumnal downwelling transitions

Study region	$Wind_{max}$	$Wind_{min}$	Upwelling start	Upwelling end
A	15.45 ± 0.93	−10.17 ± 0.46	15 Feb ± 21	5 Nov ± 7
B	15.40 ± 0.97	−11.18 ± 0.66	27 Feb ± 21	8 Nov ± 7
C	16.28 ± 1.26	−10.93 ± 0.43	21 Feb ± 19	17 Nov ± 17
D	17.55 ± 1.37	−11.78 ± 0.52	3 Mar ± 39	10 Nov ± 7
E	15.69 ± 0.89	−16.75 ± 0.40	14 Feb ± 19	7 Dec ± 6

Table 4. Maximum and minimum upwelling values from the NOAA Environmental Research Division upwelling indices (± 95% CI, as calculated from multi-year time series), and the dates (± CI, in days) at which upwelling begins and ends

Latitude (°N)	$Upwelling_{max}$	$Upwelling_{min}$	Upwelling start	Upwelling end
48	109.5 ± 7.4	−461.8 ± 29.7	4 Apr ± 27	15 Oct ± 13
45	144 ± 6	−447.2 ± 25.6	12 Mar ± 20	18 Oct ± 22
42	321.5 ± 17.2	−458.8 ± 28	5 Mar ± 21	9 Nov ± 7

Chl concentration is a proxy for phytoplankton concentrations. As mentioned previously, neither of the 2 main toxin-producing genera occurring off the Oregon coast, *Pseudo-nitzschia* and *Alexandrium*, has unique optical signatures that can be utilized by satellite, and they are often not the dominant species found in bloom assemblages. However, satellite chl observations include a contribution from toxic algal species when they are present. In this study, satellite chl provides a context within which to compare toxin concentrations and cell counts of harmful genera.

In the oceanic regions, chl was lowest in summer and highest in winter (Fig. 6a), as was also reported by Thomas et al. (1994). There was no significant difference between regions throughout the year, with the exception of Region D, which had significantly higher oceanic chl_{min} (Table 5). The timing of spring and autumnal changes in oceanic chl did not vary among regions.

In the coastal regions, chl was generally highest in summer and lowest in winter (Fig. 6b). Chl_{max} significantly decreased to the south over Regions A to E (Table 5), with the exception of Region B, which had the lowest chl_{max} values. Chl_{min} (Table 5) was significantly highest in Region A and significantly lowest in Region E, with only Regions B and C not significantly different.

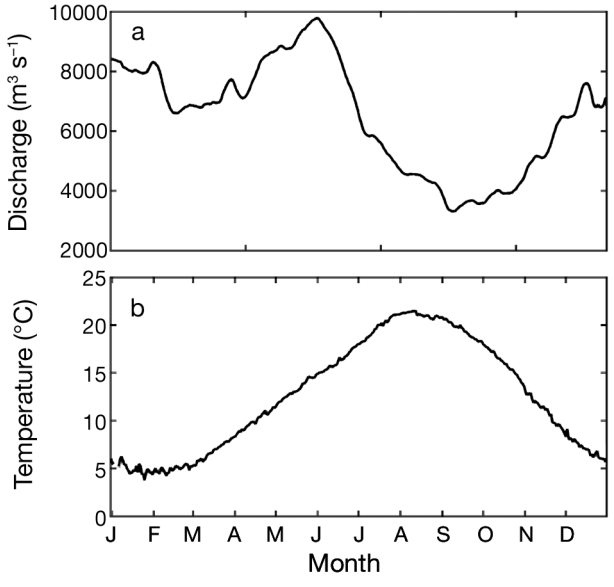

Fig. 5. Mean Columbia River (a) outflow ($m^3 s^{-1}$) and (b) temperature (°C), 1998 to 2007

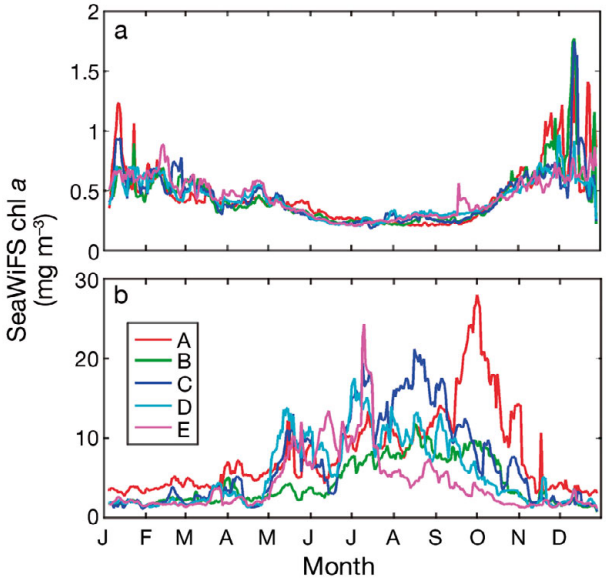

Fig. 6. Mean daily chlorophyll concentrations (chl, mg m^{-3}; SeaWiFS) from (a) oceanic and (b) coastal study regions (A to E, see Fig.1), 1998 to 2007. Note differing chl axis scales

Table 5. Maximum and minimum chlorophyll (chl, mg m^{-3}, ± 95% CI, as calculated from multi-year time series), for the oceanic and coastal regions, and timing of chl blooms (± CI, in days)

Study region	Oceanic chl_{max}	Oceanic chl_{min}	Coastal chl_{max}	Coastal chl_{min}	Spring bloom	Summer bloom
A	0.72 ± 0.09	0.16 ± 0.01	32.18 ± 3.08	3.01 ± 0.24	6 Mar ± 23	25 Apr ± 11
B	0.71 ± 0.06	0.17 ± 0.01	16.5 ± 1.21	1.53 ± 0.15	6 Mar ± 16	25 Apr ± 1
C	0.78 ± 0.08	0.16 ± 0.01	28.31 ± 2.07	1.63 ± 0.21	31 Mar ± 47	14 May ± 21
D	0.70 ± 0.04	0.18 ± 0.01	24.34 ± 2.25	1.33 ± 0.15	31 Mar ± 48	14 May ± 14
E	0.72 ± 0.72	0.17 ± 0.01	19.64 ± 2.99	1.03 ± 0.07	14 Jan ± 2	18 Apr ± 2

The onset of bloom conditions occurred between mid-March and early April (Table 5). There was no significant difference in the mean start date of the bloom between Regions A and B (6 March), and between Regions C and D (31 March). The mean start date of the bloom in Region E was 14 January. After these initial increases, chl returned to winter values before a secondary bloom associated with the onset of upwelling. The timing sequence of the upwelling bloom mirrored the first bloom (Table 5), with earliest initiation each year in Region E (18 April), followed by Regions A and B (25 April), and then Regions C and D (14 May). Maximum bloom conditions occurred around 17 August in Regions A and B, 26 June in Region C, and 27 July in Regions D and E. Concentrations of chl observed in the oceanic regions (<2 mg m^{-3}) were low compared to coastal chl (mean ~6 mg m^{-3}), and in particular to peak coastal chl (~110 mg m^{-3}). Therefore, subtraction of oceanic values from coastal chl to obtain a 'detrended' Δchl, as we did for SST, was not considered useful. Bloom initiation dates and magnitudes were not affected by 'detrending.'

The cell counts obtained from water samples at NH5 provide a connection between chl and toxins in shellfish at the coast. At NH5, situated 5 nautical miles from the coast within Region C, 5 yr of data were used to create climatologies of the potentially toxic genera *Pseudo-nitzschia* and *Alexandrium*. Typically neither of the genera was dominant within a sample, instead making up only part of the diverse community. However, *Alexandrium* spp. represented >80% of phytoplankton standing stock in August 2001, and *Pseudo-nitzschia* spp. frequently constituted over 20% of total cells and represented >50% on 4 occasions between 2001 and 2007.

Pseudo-nitzschia spp. were found throughout the year; however, mean cell concentrations were elevated between May and August (with a significant peak in June), with a second significant increase of cell densities in October (Fig. 7a). During any of these bloom periods, cell densities could reach densities above 'concern' levels of >10 000 cells l^{-1}, as defined by Howard et al. (2007).

At the coast, ODFW plankton sampling revealed regional differences in abundances of *Pseudo-nitzschia* spp. (Fig. 8). In Regions A, C, and D (B was unfortunately not sampled) *Pseudo-nitzschia* spp. cell densities were consistently highest in May. In Region A, a significant increase in May, and subsequent decrease in June, was followed by a lesser increase in July. This secondary increase occurred progressively later in Regions C (August) and D (September). In these 3 more northern regions, cell densities only exceeded 'concern' levels in May through August, although the time series is short (2005 to 2007). In the

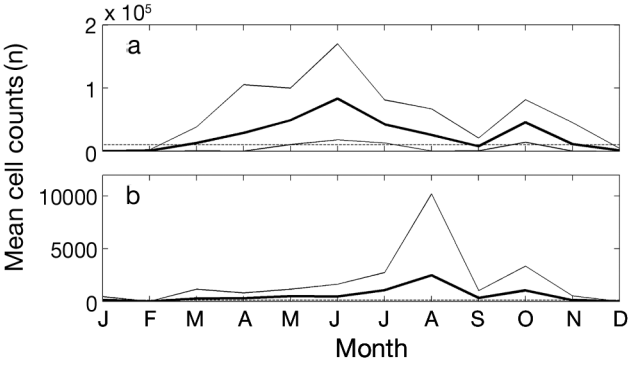

Fig. 7. Mean monthly counts of phytoplankton cells (cells l^{-1}) belonging to the genera (a) *Pseudo-nitzschia* and (b) *Alexandrium*, from surface water samples collected at site NH5 from 2001 to 2007. Thick black line shows the mean cell densities of each month, calculated over all years; thin black lines indicate the 95% confidence intervals on the mean, calculated for each month over all years using bootstrapping. Dashed line in (a) marks the 'concern' level of 10 000 *Pseudo-nitzschia* spp. cells l^{-1} (Howard et al. 2007). 'Concern' level for *Alexandrium* spp. is 100 cells l^{-1}

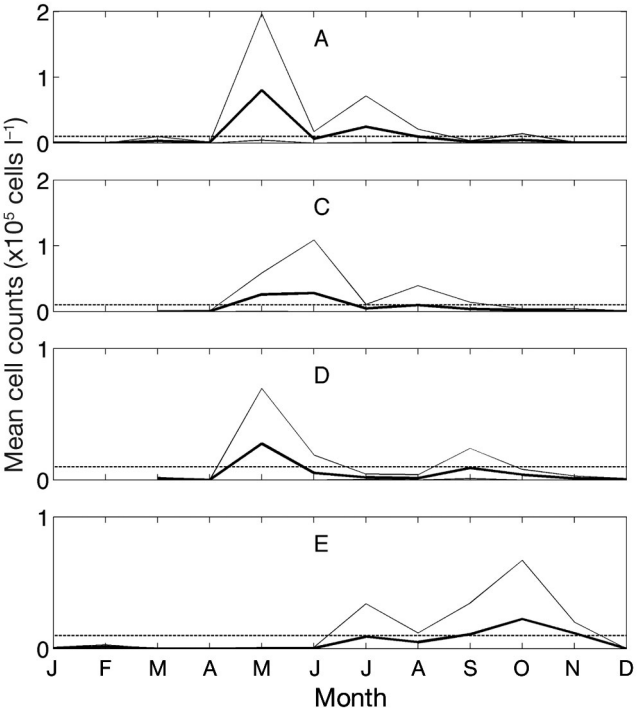

Fig. 8. Counts of phytoplankton cells (cells l^{-1}) belonging to the genus *Pseudo-nitzschia*, taken by the Oregon Department of Fish and Wildlife from 2005 to 2007 in study regions A, C, D, and E (see Fig. 1). Thick black line shows the mean cell densities of each month, calculated over all years; thin black lines indicate the 95% confidence intervals on the mean, calculated for each month over all years using bootstrapping. Dashed line marks the 'concern' level of 10 000 cells l^{-1} (Howard et al. 2007). Note differing cell count axis scales

southernmost Region, E, *Pseudo-nitzschia* spp. cell densities remained low until July, with increased concentrations lasting into November.

Off the coast, at NH5, *Alexandrium* spp. are also found throughout the year, although at very low densities in November through to February. Mean cell densities increased in August, with maximum observed concentrations over an order of magnitude higher than those observed in all other months (Fig. 7b). However, *Alexandrium* spp. were found only twice out of 298 samples in the ODFW coastal sampling: 2000 cells l^{-1} on 1 January 2006 in Region A, and 5000 cells l^{-1} on 6 August 2006 in Region B. Both instances were above the warning levels of 100 cells l^{-1}, the 'concern' level used by the ODFW.

Both domoic acid and saxitoxin concentrations showed temporal and spatial variations in the ODA shellfish samples. Domoic acid could be found in shellfish throughout the year in all regions, though not in every year. Region A showed a highly significant peak in domoic acid concentrations in October (Fig. 9) and low toxin concentrations between May and August. Mean toxin concentrations were generally higher in this region, except for May to August. These increased mean concentrations were reflected in more shellfish harvesting closures in Region A compared to other regions. Mean domoic acid concentrations were highest in May in Regions B, C, D, and E (Fig. 9), with highest peak concentrations in May and June. For the rest of the year, increased domoic acid concentrations occurred in Regions C (September–October), D (September–November), and E (February and October). There were small peaks in the frequency of shellfish bed closures associated with the periods of increased mean domoic acid concentrations.

Saxitoxin was found throughout the year in all regions (Fig. 10), though only in region A were discrete sample concentrations exceeding closure levels found in all months (data not shown). In Regions B, C, and E, a significant peak in concentrations was observed later in the year (September/October, September, and August, respectively).

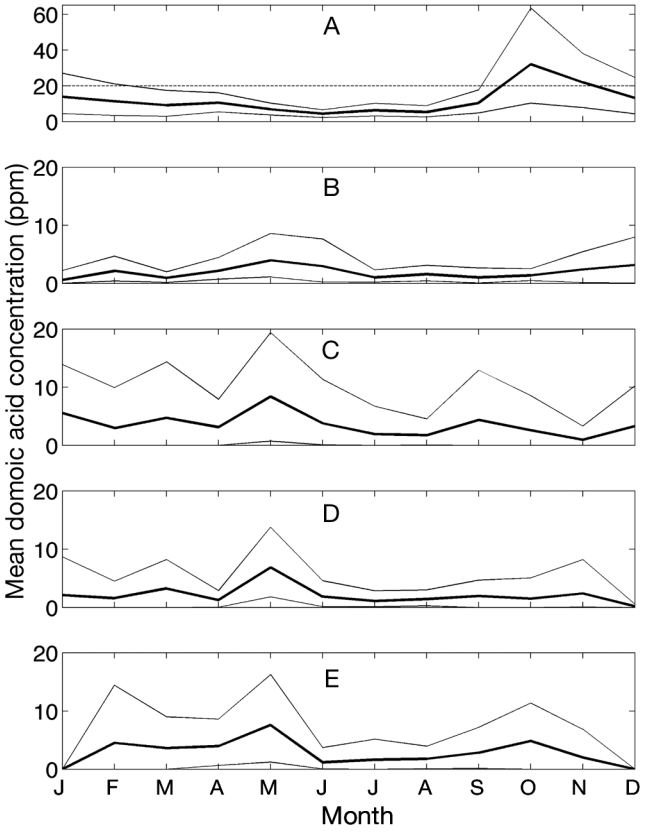

Fig. 9. Domoic acid concentrations in shellfish (ppm), 1994 to 2007, in study regions A to E (see Fig. 1). Thick black line represents the mean cell densities each month, calculated over all years; thin black lines indicate the 95% confidence intervals of the mean, calculated for each month over all years using bootstrapping. Dashed line marks the closure level of 20 ppm. Note differing toxin concentration axis scales

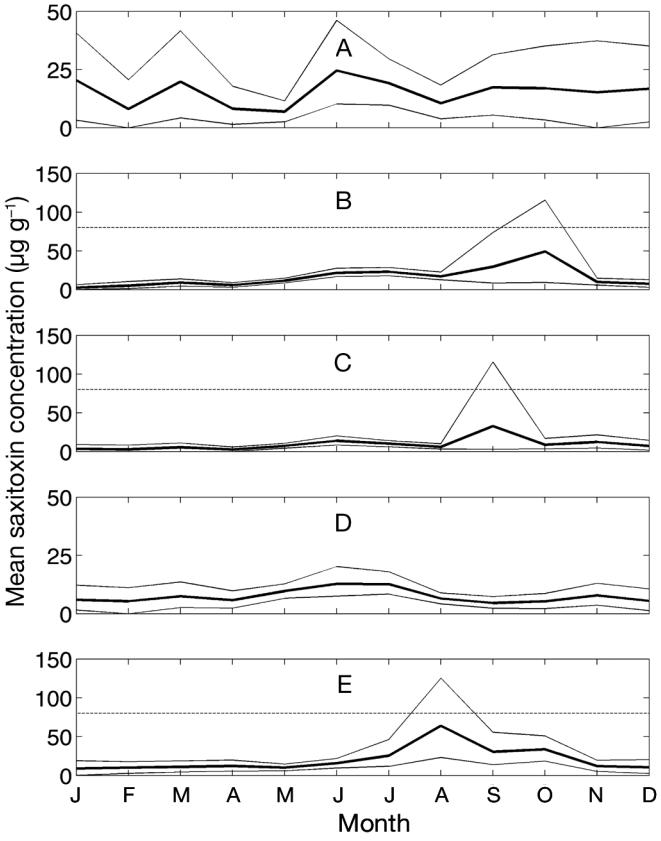

Fig. 10. Saxitoxin concentrations in shellfish (µg 100 g^{-1}), 1979 to 2007, in study regions A to E (see Fig. 1). Thick black line represents the mean cell densities each month, calculated over all years; the thin black lines indicate the 95% confidence intervals of the mean, calculated for each month over all years using bootstrapping. Dashed line marks the closure level of 80 µg 100 g^{-1}. Note differing toxin concentration axis scales

DISCUSSION

Physical oceanography

Coastal Oregon physical and biological oceanographic variability is dominated by seasonally alternating upwelling and downwelling, driven by alongshore winds (Huyer et al. 1979, Thomas & Strub 1989, Thomas et al. 1994, Henson & Thomas 2007). As such, a clear understanding of temporal and spatial variability in upwelling timing and strength along the Oregon coast is important for understanding physical drivers of Oregon HAB events. The wind data presented here corroborate the work of Henson & Thomas (2007), i.e. upwelling favorable winds occur after late February each year. A latitudinal gradient in winds and in the onset and intensity of upwelling has been noted for the California Current System (Strub et al. 1987a,b, Largier et al. 1993, Strub & James 2000, Samelson et al. 2002), but previous studies have not looked in detail at the Oregon coast and thus have potentially missed smaller-scale spatial patterns.

For Regions A through D, the calculated start date of upwelling was dependent on whether it was calculated from the wind climatology or from individual years, and then averaged. This was because in these 4 regions, wind direction was variable and not uniformly upwelling favorable during spring in individual years. The wind climatology therefore reflects when winds have become more consistently upwelling favorable in all years. There was no difference between the start of upwelling calculated from yearly dates and wind climatology in Region E. This was due to the more steady southward direction of the winds in this area throughout the spring and summer. There is a change in wind, and hence upwelling, climatology around Cape Blanco (42.84° N, between the coastal Regions D and E; Samelson et al. 2002, Huyer et al. 2005, Venegas et al. 2008). North of Cape Blanco there was no significant difference in the timing of the upwelling season, but south of Cape Blanco upwelling favorable winds started significantly earlier and finished significantly later.

The strength of the upwelling index at 45° N was directly proportional to the strength of the north–south wind vector within Regions B and C ($r^2 = 0.53$ and 0.58, respectively, $p < 0.05$). The strength of upwelling in Regions A and D could not be compared to wind strength with the present data set due to the low spatial resolution of the upwelling index; however, the mean start date of upwelling as indicated by upwelling favorable winds within Regions A, B, C, and D and the 45° N upwelling index were not significantly different. It therefore appears that the single 45° N upwelling index is a good indicator of whether upwelling is occurring along the Oregon coast between the Oregon/Washington border and Cape Blanco. South of Cape Blanco, the mean start date of upwelling favorable winds in Region E was not significantly different from the beginning of upwelling according to the 42° N upwelling index, and throughout the year, the strength of the upwelling index was directly proportional to the strength of the north–south wind vector ($r^2 = 0.61$, $p < 0.05$).

While the upwelling index is useful for determining the timing of upwelling, the 3° latitude spacing provides poor information on the strength of upwelling at the latitudes between. The wind climatology suggests similar upwelling patterns in Regions B, C, and D, stronger upwelling over a longer period in Region E (as seen in the upwelling indices), and weaker upwelling, due to significantly lower wind speeds, in Region A. The coastal detrended SST provides a relative measure of upwelling strength, with larger negative values indicative of stronger upwelling. As expected, ΔSST was lower for a longer interval in Region E, compared to all other regions. North of Cape Blanco, however, Region B ΔSST was not significantly different from Region A, and was significantly weaker than Regions C and D, with which Region B shared similar wind climatology.

Thomas & Weatherbee (2006) found that the plume of the Columbia River, which is warmer than the surrounding ocean waters in summer, extends southward in summer, in some cases including Region B as well as Region A. Thus, the southward extension of the river plume may be raising the SST of Regions A and B through the presence of the warmer river plume water, masking the extent of upwelling as quantified by ΔSST.

Chlorophyll phenology

Although the genera of the harmful algae found off the Oregon coast have no unique optical signatures, they do contribute to SeaWiFS chl data. The first of the 2 annual phytoplankton blooms observed in the satellite chl data in all regions occurred before upwelling lowered SST. Light supply to phytoplankton is a balance between mixed layer depth and irradiance. Light has been found to be limiting on the Oregon shelf at 45° N in January (Wetz et al. 2004), and north of ~46° N, light is limiting until mid-March (Henson & Thomas 2007). At ~40° N, Thomas & Strub (1989) suggested that light would likewise be limiting until mid-March, while Henson & Thomas (2007) found that light levels were unlikely to be limiting to phytoplankton growth south of ~40° N. S. Henson (pers. comm.) calculated the boundary between seasonally light limited and non-light limited areas for 2002 to 2007, using optimally interpolated Argo float data to estimate

mixed layer depth and SeaWiFS PAR and K_{490} (as in Eq. 1 of Henson & Thomas 2007), where PAR is photosynthetically active radiation, K_{490} indicates the turbidity of the water column, and light limitation is considered as depth-averaged irradiance <21 W m^{-2} in accordance with Riley (1957). The latitude at which light became limiting varied interannually between ~40 and 45° N, and extended as far south as 37° N in 2003. The smaller, earlier bloom along the Oregon coast in March therefore appears to be a spring bloom, as seen in other temperate regions, occurring when light limitation in the surface mixed layer is relieved.

Although Regions A and B are farther north than Regions C and D, and therefore receive lower daily irradiance in March, their earlier spring bloom start date may be due to the effect of the Columbia River plume. The Columbia River outflow is high in March, and at the same time the plume begins to extend south and offshore rather than northward (Thomas & Weatherbee 2006) due to wind forcing. Thomas & Weatherbee (2006) found increased suspended particulate material (SPM) concentration in the Columbia River plume, compared to surrounding waters, which could result in over-estimation of chl values. However, the Columbia River may provide nutrients such as silicic acid (Haertel et al. 1969, Aguilar-Islas & Bruland 2006) to the shelf waters, and also potentially creates a shallow, fresher surface mixed layer, therefore relieving surface mixed layer light limitation earlier, leading to earlier increases in primary production. The chl time series data show that the spring bloom declines after about 2 wk. This is due to nutrient depletion, as zooplankton biomass, and so grazing rates, are usually low during this time (Peterson & Keister 2003).

Relationships to harmful algal blooms

SeaWiFS chl data are from the upper 10 m or less in coastal regions, and are not reliable within a few kilometers of the coast (these data are masked in NASA's processing). Consequently, ocean color measurements are possibly separated in the vertical and horizontal from surf zone cell densities and toxin concentrations, potentially limiting analysis. However, the purpose of this research was to investigate linkages between easily observed environmental parameters, such as SST and chl, and appearances of algal toxins at the coast. These comparisons are particularly useful in looking at larger scales (~100 km). Furthermore, the data from SeaWiFS, or similar products from other ocean color sensors such as the Moderate Resolution Imaging Spectrometer (MODIS Aqua), and in the future the Medium Resolution Imaging Spectrometer (MERIS), can be obtained cheaply from NASA and NOAA, cost being an important consideration in the viability of a long-term HAB monitoring scheme. Data from site NH5 provided a link between shore-based data and chl values away from the coast.

The March spring bloom increase in chl did not correspond to increased counts of *Pseudo-nitzschia* spp. at NH5 or the coast, or to increased occurrences of domoic acid in shellfish. Huyer et al. (2007) reported the dominance of the diatoms of the genera *Thalassiosira* Cleve, *Actinoptychus* Ehrenberg, and *Asterionellopsis* Round in the spring bloom at 45.6° N, off Oregon. Species of the genus *Pseudo-nitzschia* are not normally dominant, even when present in high numbers. Mean cell densities of the genus *Alexandrium* did not show a significant increase in March at NH5, and no significant increase in saxitoxin concentrations were seen at the coast. Thus, the spring bloom does not appear to be particularly associated with the presence of potentially toxic algal genera, at the Oregon coast, or 5 nautical miles offshore.

A second phytoplankton bloom begins in Regions C, D, and E in April/May each year. It is generated by upwelling, occurs about 2 wk after coastal SST begins cooling, and extends into the summer. The initial period of this second bloom was associated with increased *Pseudo-nitzschia* spp. cell densities offshore at NH5, reaching peak densities in June, with peak *Alexandrium* spp. cell densities in August, suggesting an ecological succession of HAB species through the period of elevated summer chl concentrations. This period also corresponded to increasing cell densities of *Pseudo-nitzschia* spp. in the coastal cell counts in Regions C and D, peaking in May, though present in low densities throughout the rest of the summer upwelling period. In Region D, warning levels of *Pseudo-nitzschia* spp. were only exceeded in May. May also corresponded to the maximum concentrations of domoic acid in shellfish in Regions C, D, and E. The bi-weekly sampling for cell counts, and the unevenness of the shellfish tissue sampling frequencies, did not allow for investigation into latitudinal gradients at less than monthly time scales, in comparison to the daily to weekly oceanic parameters sampled by satellite.

In Regions A and B, the second phytoplankton bloom started in April when winds were upwelling favorable, but before coastal SST cooled due to upwelling. During this time, coastal SST in Regions A and B was correlated closely with Columbia River temperatures, suggesting a surface layer of river plume water. In Region A, cell densities of *Pseudo-nitzschia* spp. began to increase in April, and were the highest of all sampled regions. Region A also had the greatest proportion of toxin samples over closure levels. Unfortunately, Region B was not sampled by the ODFW for cell

counts. The smaller proportion of shellfish tissue toxin samples exceeding closure levels in Region B, in comparison to Region A, suggests that cell densities of *Pseudo-nitzschia* spp. may have been lower than in Region A, or cells were not as toxic.

During the majority of the upwelling season, instances of detectable domoic acid concentrations occurred in all regions but remained relatively low. In Region A, which contains Clatsop Beach where most of the Oregon recreational and commercial razor clam harvest is concentrated, shellfish samples were contaminated with domoic acid more often than other regions, but concentrations were lowest during the summer. Not all species of *Pseudo-nitzschia* worldwide produce domoic acid, and those that do — e.g. *P. australis* Frenguelli, *P. multiseries* (Hasle) Hasle, *P. delicatissima* (Cleve) Heiden, *P. pseudodelicatissima* (Hasle) Hasle, *P. seriata* (Cleve) Peragallo — are not consistently toxic. Toxin production has been associated with nutrient limitation (Pan et al. 1996a,b, Maldonado et al. 2002, Fehling et al. 2004), and since upwelling supplies nutrients to the coastal regions, high concentrations of domoic acid would not necessarily be expected during upwelling. Trainer et al. (2009) found no consistent relationship between nutrient concentrations, or nutrient ratios, and domoic acid concentrations.

However, the greater likelihood of domoic acid in shellfish in Region A, where *Pseudo-nitzschia* spp. concentrations were not much different from other regions, suggests that nutrient stress may be a factor in this region. As discussed above, the Columbia River plume does contain nutrients and may act as a significant source at certain times of the year, but in general it contains lower nutrient concentrations than recently upwelled shelf water (Haertel et al. 1969, Aguilar-Islas & Bruland 2006) and forms a surface layer in Regions A and B. The toxic *Pseudo-nitzschia* spp. may also be advected in from other areas, such as the Washington coast to the north. Trainer et al. (2002) emphasized the importance of the Juan de Fuca eddy for the initiation of toxic *Pseudo-nitzschia* spp. blooms off the Washington coast. It was hypothesized that the eddy acts as a 'bioreactor,' whereby blooms are maintained offshore in the eddy throughout the summer, then brought onshore by changes in the wind field associated with either episodic storm events, or the transition from summer upwelling to winter downwelling in September/October. Modeling studies (MacFadyen et al. 2005) and analyses of ocean color satellite data (Sackmann & Perry 2006) have both confirmed the importance of the Juan de Fuca eddy as a source of Washington shelf waters.

Domoic acid concentrations in all regions were most likely to lead to closures at the start of the summer bloom, or at the end of the upwelling season in autumn. The switch to downwelling would work in 2 ways to increase domoic acid concentrations in shellfish on the coast, firstly by decreasing nutrient supply to *Pseudo-nitzschia* spp., hence potentially stimulating toxin production, and secondly by bringing the toxic *Pseudo-nitzschia* spp. towards the coast. Thus a clear understanding of temporal and spatial patterns of upwelling is necessary for HAB studies and coastal management along the Oregon coast. At the start of the upwelling season and during the summer bloom, particularly north of Cape Blanco, winds are variable and switch frequently between upwelling and downwelling favorable. Monitoring of coastal winds, along with surface currents measured by high frequency radar (http://bragg.oce.orst.edu), could be used to predict or monitor onshore currents and give some warning to coastal managers of potential HAB events. In the near future, circulation models could be used to predict the trajectory of blooms 2 or more days into the future.

Saxitoxin concentrations did not show a significant response to the start of the summer bloom in any of the 5 regions. Increases in mean toxin concentrations were observed later in summer and early autumn, though still during the upwelling season. The highest proportions of samples leading to closures also occurred during the upwelling season, although closures due to saxitoxin were rarer than those due to domoic acid. Just as the summer bloom begins progressively later from south to north along the Oregon coast, so does the peak of saxitoxin concentration. This is consistent with a change in phytoplankton community structure, as suggested by the NH5 cell count sample analysis described above.

Phytoplankton of the genus *Alexandrium* form resting cysts that reside in the sediments (Anderson & Wall 1978). These cysts germinate annually (Matrai et al. 2005) and provide a seed population for a bloom. Anderson et al. (2005b) found that light and higher temperatures enhanced germination of *Alexandrium* cysts, whereas Perez et al. (1998) found no correlation with temperature. Nishitani & Chew (1984) found that growth rates were increased above a threshold temperature of 13°C. Upwelling could be bringing germinated cysts, or cysts within the water column (Kirn et al. 2005), to the surface and provide a source of *Alexandrium* spp. and hence saxitoxin along the Oregon coast. In 2006, sediment grab samples were collected by our group (Scott 2007) in 3 estuaries (Tillamook Bay, Region B; Yaquina Bay, Region C; Coos Bay, Region D) and from 3 open water transects (off Newport, Seal Rock, and Strawberry Hill, all Region C). Samples were processed according to Anderson et al. (1982). Less than 10 cysts in total were found, compared to the hundreds cm^{-3} of sediment routinely observed in the Gulf of Maine (Anderson et al.

2005a,b). Very few *Alexandrium* spp. cells have been observed within our small database of cell counts; however, the presence of saxitoxin in shellfish tissues suggests that our sampling may have been inadequate, or that the source of *Alexandrium* is outside of Oregon waters, perhaps to the north. Cox et al. (2008) found that sediment cyst concentrations were not always a good indicator of saxitoxin in shellfish. *Alexandrium* spp. cell abundances as low as 100 cells l^{-1} (Lassus et al. 1994), which may be below the sensitivity of our cell counts, can potentially produce saxitoxin concentrations above detection limits.

The concentrations of domoic acid in shellfish samples decreased through the summer, and into winter and spring of the following year, indicative of slow depuration from tissues, rather than exposures to a new toxin source. Depuration rates of domoic acid and saxitoxin out of shellfish tissues vary with shellfish species (Bricelj & Shumway 1998) and toxin, and our work considers all sampled shellfish species as 1 data set. Although this may 'blur' the signal of individual toxic events, the grouping of all species accurately represents the spatial and temporal occurrence of toxins and the oceanographic conditions associated with toxicity, and the threat to human health. Interannual variability in shellfish toxin concentrations is also an important consideration. Future publications will quantify this variability and investigate individual events in more detail.

CONCLUSIONS

Region A, which contains the Columbia River plume, is a 'hotspot' for domoic acid. Concentrations of *Pseudo-nitzschia* spp. are higher during the summer upwelling season in this area than along the rest of the Oregon coast. Domoic acid concentrations in coastal shellfish are associated with downwelling transitions, which are characterized by shelf waters being brought to the coast and potentially experiencing nutrient stress at the end of a bloom. Although *Alexandrium* spp. were rarely seen at the coast during our short (3 yr) time series of phytoplankton counts, saxitoxin could be found in any month along the Oregon coast based on the longer (1979 to 2007) toxin database. Saxitoxin concentrations were highest during times of upwelling, particularly late summer.

These results provide a framework to guide sampling strategies for coastal managers. Region A is a high risk region for domoic acid in shellfish and should be a priority in shellfish sampling, particularly due to the large shellfish harvesting activities in that region. The start of summer upwelling, with associated springtime short relaxation and downwelling events, and the autumn downwelling transition are associated with increased domoic acid concentrations at the coast. Upwelling periods are associated with saxitoxin fisheries closures. These oceanographic events (summer phytoplankton bloom, transitions from upwelling to downwelling) are easily identifiable by satellites and *in situ* data products (such as upwelling from AVHRR SST images, available free from the CoastWatch West Coast Regional Node, http://coastwatch.pfeg.noaa.gov/coastwatch/CWBrowser.jsp). Regular sampling will be important in determining when fisheries can open again, as shellfish take time to depurate toxin from their tissues, and this may not be coincidental with changes in oceanic conditions. Grouping all toxin data into 5 regions has identified latitudinal gradients in physics, biology, and toxin events, but has removed details on where exactly within those regions closures occur, for example open coast or in estuaries. Further work may be able to pinpoint individual hotspot sites and specify detailed sequences of oceanographic conditions leading to closure events. Our ultimate goal is monitoring via satellite for potential events and providing early warning to coastal managers, rather than the general phenology of potentially toxic genera presented here. The relationships between phycotoxins and oceanographic conditions, observable by satellite, are fairly consistent between years, providing an additional tool to Oregon's coastal managers in planning sampling strategies and protecting public health.

Acknowledgements. We thank S. Henson for helpful comments on an earlier version of the manuscript. This study was supported by NOAA grants NA04OAR4600202 from the Oceans and Human Health Initiative, NA07NOS4780195 from the Monitoring and Event Response for Harmful Algal Blooms (MERHAB) program and NA08NES4400013 to the Cooperative Institute for Oceanographic Satellite Studies. The statements, findings, conclusions, and recommendations are those of the author(s) and do not necessarily reflect the views of the National Oceanic and Atmospheric Administration or the Department of Commerce. This is MERHAB publication no, 65. AVHRR SST data were provided by NOAA CoastWatch. QuikSCAT wind data were provided by the Physical Oceanography Distributed Active Archive Center at NASA's Jet Propulsion Laboratory (California Institute of Technology). SeaWiFS data were provided courtesy of NASA's Goddard Space Flight Center and Geoeye Inc.

LITERATURE CITED

Adams NG, Lesoing M, Trainer VL (2000) Environmental conditions associated with domoic acid in razor clams on the Washington coast. J Shellfish Res 19:1007–1015

Aguilar-Islas AM, Bruland KW (2006) Dissolved manganese and silicic acid in the Columbia River plume: a major source to the California current and coastal waters off Washington and Oregon. Mar Chem 101:233–247

Anderson DM, Wall D (1978) Potential importance of benthic cysts of *Gonyaulax tamarensis* and *G. excavata* in initiating toxic dinoflagellate blooms. J Phycol 14:224–234

Anderson DM, Aubrey DG, Tyler MA, Coats DW (1982) Vertical and horizontal distributions of dinoflagellate cysts in sediments. Limnol Oceanogr 7:757–765

Anderson DM, Keafer BA, McGillicuddy DJ Jr, Mickelson MJ and others (2005a) Initial observations of the 2005 *Alexandrium fundyense* bloom in southern New England: general patterns and mechanisms. Deep-Sea Res II 52: 2856–2876

Anderson DM, Stock CA, Keafer BA, Nelson AB and others (2005b) *Alexandrium fundyense* cyst dynamics in the Gulf of Maine. Deep-Sea Res II 52:2522–2542

Anderson DM, Burkholder JM, Cochlan WP, Glibert PM and others (2008) Harmful algal blooms and eutrophication: examining linkages from selected coastal regions of the United States. Harmful Algae 8:39–53

AOAC (Association of Official Analytical Chemists) (1990) Official methods of analysis of the Association of Official Analytical Chemists, 15th edn. AOAC, Arlington, VA

Barth JA, Wheeler PA (2005) Introduction to special section: coastal advances in shelf transport. J Geophys Res 110: C10S01 doi:10.1029/2005JC003124

Bricelj V, Shumway SE (1998) Paralytic shellfish toxins in bivalve molluscs: occurrence, transfer kinetics, and biotransformation. Rev Fish Sci 6:315–383

Cox AM, Shull DH, Horner RA (2008) Profiles of *Alexandrium catenella* cysts in Puget Sound sediments and the relationship to paralytic shellfish poisoning events. Harmful Algae 7:379–388

Efron B, Gong G (1983) A leisurely look at the bootstrap, the jackknife, and cross-validation. Am Stat 37:36–48

Fehling J, Davidson K, Bolch CJ, Bates SS (2004) Growth and domoic acid production by *Pseudo-nitzschia seriata* (Bacillariophyceae) under phosphate and silicate limitation. J Phycol 40:674–683

Fryxell GA, Villac MC, Shapiro LP (1997) The occurrence of the toxic diatom genus *Pseudo-nitzschia* (Bacillariophyceae) on the west coast of the USA, 1920–1996: a review. Phycologia 36:419–437

Glibert PM, Seitzinger S, Heil CA, Burkholder JM, Parrow MW, Codispoti LA, Kelly V (2005) The role of eutrophication in the global proliferation of harmful algal blooms. Oceanography 18:198–209

Haertel L, Osterberg C, Curl H Jr, Park PK (1969) Nutrient and plankton ecology of the Columbia River Estuary. Ecology 50:962–978

Henson SA, Thomas AC (2007) Interannual variability in timing of bloom initiation in the California Current System. J Geophys Res 112:C08007 doi:10.1029/2006JC 003960

Henson SA, Robinson I, Allen JT, Waniek JJ (2006a) Effect of meteorological conditions on interannual variability in timing and magnitude of the spring bloom in the Irminger Basin, North Atlantic. Deep-Sea Res I 53:1601–1615

Henson SA, Sanders R, Holeton C, Allen JT (2006b) Timing of nutrient depletion, diatom dominance and a lower-boundary estimate of export production for Irminger Basin, North Atlantic. Mar Ecol Prog Ser 313:73–84

Horner RA (2001) *Alexandrium* and *Pseudo-nitzschia*: two of the genera responsible for harmful algal blooms on the U.S. west coast. In: RaLonde R (ed) Harmful algal blooms on the North American west coast. University of Alaska Sea Grant, AK-SG-01-05, Fairbanks, p 5–10

Horner RA, Garrison DL, Plumley FG (1997) Harmful algal blooms and red tide problems on the U.S. west coast. Limnol Oceanogr 42:1076–1088

Howard MDA, Cochlan WP, Ladizinsky N, Kudela RM (2007) Nitrogenous preference of toxigenic *Pseudo-nitzschia australis* (Bacillariophyceae) from field and laboratory experiments. Harmful Algae 6:206–217

Huyer A, Sobey EJC, Smith RL (1979) The spring transition in currents over the Oregon continental shelf. J Geophys Res 84:6995–7011

Huyer A, Fleischbein JH, Keister J, Kosro PM, Perlin N, Smith RL, Wheeler PA (2005) Two coastal upwelling domains in the northern California Current system. J Mar Res 63: 901–929

Huyer A, Wheeler PA, Strub PT, Smith RL, Letelier R, Kosro PM (2007) The Newport line off Oregon — studies in the North East Pacific. Prog Oceanogr 75:126–160

Kahru M, Mitchell BG (2008) Ocean color reveals increased blooms in various parts of the World. EOS Trans Am Geophys Union 89:170

Kahru M, Kudela RM, Manzano-Sarabia M, Mitchell BG (2009) Trends in primary production in the California Current detected with satellite data. J Geophys Res 114: C02004 doi:10.1029/2008JC004979

Kirn SL, Townsend DW, Pettigrew NR (2005) Suspended *Alexandrium* spp. hypnozygote cysts in the Gulf of Maine. Deep-Sea Res II 52:2543–2559

Landsberg JH (2002) The effects of harmful algal blooms on aquatic organisms. Rev Fish Sci 10:113–390

Largier JL, Magnell BA, Winant CD (1993) Subtidal circulation over the Northern California shelf. J Geophys Res 98: 18147–18179

Lassus P, Ledoux M, Bardouil M, Bohec M, Erard E (1994) Kinetics of *Alexandrium minutum* Halim toxin accumulation in mussels and clams. Nat Toxins 2:329–333

MacFadyen A, Hickey BM, Foreman MGG (2005) Transport of surface waters from the Juan de Fuca eddy region to the Washington coast. Cont Shelf Res 25:2008–2021

Maldonado MT, Hughes MP, Rue EL, Wells ML (2002) The effect of Fe and Cu on growth and domoic acid production by *Pseudo-nitzschia multiseries* and *Pseudo-nitzschia australis.* Limnol Oceanogr 47:515–526

Matrai P, Thompson B, Keller M (2005) Circannual excystment of resting cysts of *Alexandrium* spp. from eastern Gulf of Maine populations. Deep-Sea Res II 52:2560–2568

Nishitani L, Chew KK (1984) Recent developments in paralytic shellfish poisoning research. Aquaculture 39: 317–329

Pan Y, Rao DVS, Mann KH (1996a) Changes in domoic acid production and cellular chemical composition of the toxigenic diatom *Pseudo-nitzschia multiseries* under phosphate limitation. J Phycol 32:371–381

Pan Y, Subba Rao DV, Mann KH, Brown RG, Pocklington R (1996b) Effects of silicate limitation on production of domoic acid, a neurotoxin, by the diatom *Pseudo-nitzschia multiseries* I. Batch culture studies. Mar Ecol Prog Ser 131:225–233

Parsons ML, Dortch Q (2002) Sedimentological evidence of an increase in *Pseudo-nitzschia* (Bacillariophyceae) abundance in response to coastal eutrophication. Limnol Oceanogr 47:551–558

Perez CC, Roy S, Levasseur M, Anderson DM (1998) Control of germination of *Alexandrium tamarense* (Dinophyceae) cysts from the lower St. Lawrence Estuary (Canada). J Phycol 34:242–249

Peterson WT, Keister JE (2003) Interannual variability in copepod community composition at a coastal station in the northern California Current: a multivariate approach. Deep-Sea Res II 50:2499–2517

Riley GA (1957) Phytoplankton of the north central Sargasso Sea. Limnol Oceanogr 2:252–270

Sackmann B, Perry MJ (2006) Ocean color observations of a

surface water transport event: implications for *Pseudo-nitzschia* on the Washington coast. Harmful Algae 5: 608–619

Samelson R, Barbour P, Barth J, Bielli S and others (2002) Wind stress forcing of the Oregon coastal ocean during the 1999 upwelling season. J Geophys Res 107:3034 doi: 10.1029/2001JC000900

Scholin CA, Gulland F, Doucette GJ, Benson S and others (2000) Mortality of sea lions along the central California coast linked to a toxic diatom bloom. Nature 403:80–84

Scott BA (2007) The relationship between upwelling, shellfish toxicity, and the distribution of toxic cysts in Oregon. MSc thesis, University of Oregon, Eugene, OR

Shumway SE (1990) A review of the effects of algal blooms on shellfish and aquaculture. J World Aquacult Soc 21: 65–104

Siegel DA, Doney SC, Yoder JA (2002) The North Atlantic spring phytoplankton bloom and Sverdrup's critical depth hypothesis. Science 296:730–733

Smayda TJ (2007) Reflections on the ballast water dispersal–harmful algal bloom paradigm. Harmful Algae 6: 601–622

Strub PT, James C (2000) Altimeter-derived variability of surface velocities in the California Current System. 2. Seasonal circulation and eddy statistics. Deep-Sea Res II 47: 831–870

Strub PT, Allen JS, Huyer A, Smith RL (1987a) Large-scale structure of the spring transition in the coastal ocean off western North America. J Geophys Res 92:1527–1544

Strub PT, Allen JS, Huyer A, Smith RL (1987b) Seasonal cycles of currents, temperature, winds, and sea level over the Northeast Pacific continental shelf: 35° N to 48° N. J Geophys Res 92:1507–1526

Thomas AC, Strub PT (1989) Interannual variability in phytoplankton pigment distribution during the spring transition along the west coast of North America. J Geophys Res 94:18095–18117

Thomas AC, Weatherbee RA (2006) Satellite-measured temporal variability of the Columbia River plume. Remote Sens Environ 100:167–178

Thomas AC, Huang F, Strub PT, James C (1994) Comparison of the seasonal and interannual variability of phytoplankton pigment concentrations in the Peru and California Current systems. J Geophys Res 99:7355–7370

Trainer VL, Hickey BM, Horner RA (2002) Biological and physical dynamics of domoic acid production off the Washington coast. Limnol Oceanogr 47:1438–1446

Trainer VL, Hickey BM, Lessard EJ, Cochlan WP and others (2009) Variability of *Pseudo-nitzschia* and domoic acid in the Juan de Fuca eddy region and its adjacent shelves. Limnol Oceanogr 54:289–308

Venegas RM, Strub PT, Beier E, Letelier R and others (2008) Satellite-derived variability in chlorophyll, wind stress, sea surface height, and temperature in the northern California Current System. J Geophys Res 113:C03015 doi: 10.1029/2007JC004481

Wetz MS, Wheeler PA, Letelier RM (2004) Light-induced growth of phytoplankton collected during the winter from the benthic boundary layer off Oregon, USA. Mar Ecol Prog Ser 280:95–104

Wood AM, Apelian N, Shapiro LS (1993) Novel toxic phytoplankton: a component of global climate change? In: Guerrero R, Pedros-Alio C (eds) Trends in microbial ecology. Spanish Society of Microbiology, Barcelona, p 479–482

Editorial responsibility: Matthias Seaman, Oldendorf/Luhe, Germany

Submitted: April 2, 2009; Accepted: January 18, 2010
Proofs received from author(s): April 4, 2010